



Development and application of a simplified biophysical model to study deltaic and coastal ecosystems

Ahmed M. Khalifa^{a,*}, Ehab A. Meselhe^a, Kelin Hu^a, Denise Reed^b, Md Nazmul Azim Beg^a

^a Department of River-Coastal Science and Engineering, Tulane University, LA, USA

^b University of New Orleans, LA, USA

ARTICLE INFO

Keywords:

Hydrodynamics
Morphodynamics
Landscape evolution
Deltaic growth
Sediment diversions
Numerical modeling

ABSTRACT

Many coastal regions around the globe experience land loss due to high relative sea level rise rates, declining sediment supply, and a host of other anthropogenic factors. To evaluate possible restoration strategies, we developed a computationally efficient Simplified Biophysical Model (SBM). The SBM includes hydrodynamic, morphodynamic, and marsh inundation components. The hydrodynamic and mineral sediment processes of the SBM are based on open source Delft3D models. The marsh inundation MATLAB module is a simplified vegetation response to salinity and inundation used to estimate annual organic accretion rates. Organic accretion is added annually to the morphodynamic calculations of mineral sediment. The typical run time for the SBM for an area of 4500 km² is ~0.8, 2.5, and 4.7 days real time for one, three, and five decade simulations, respectively which is considered a computationally efficient for modeling decadal landscape evolution. The utility of the SBM was demonstrated through an application to assess the performance of a sediment diversion in the Barataria Basin in Louisiana, USA. The model results demonstrate the importance of incorporating the impact of salinity and inundation effects on the resilience of marshes subjected to high rates of relative sea level rise. Further, the sediment reduction analysis confirms the critical impact of the Mississippi River sediment decline on potential land building from sediment diversions where 1.5%, and 3% annual declining rates show a reduction in net land gain due to Mid-Barataria Sediment Diversion operation of 30% and 50 %, respectively. This highlights the importance of considering the Mississippi River sediment supply decline in restoration projects' planning and specifically, sediment diversions.

1. Introduction

Relative sea level rise (RSLR), the combination of sea level rise (SLR) and subsidence is impacting many coastal regions (Crossland et al., 2005; Huu Nguyen et al., 2016; Chen et al., 2021). Numerous deltaic systems are experiencing severe environmental impacts from RSLR resulting in varying levels of vulnerability (Sušnik et al., 2015; Huu Nguyen et al., 2016; Takagi et al., 2016; Abutaleb et al., 2018; Vu et al., 2018; Parker, 2020; Chen et al., 2021). Each delta is unique regarding processes, their complex feedbacks and resulting impact on the deltaic system (Crossland et al., 2005; Hu et al., 2021). For example, marsh transitions over time (Reed et al., 2020) respond to factor including relative sea level rise (RSLR) (Kirwan and Temmerman, 2009; Kirwan et al., 2010), storm patterns (Schuerch et al., 2013), salinity, tidal regime, inundation (depth, frequency, and duration) (Reed and Cahoon, 1992; Rozas and Reed, 1993; Cahoon and Reed, 1995), meteorological

forces, marsh edge erosion (Reed et al., 2020; Lauzon and Murray, 2022), nutrient availability, biomass distribution, seedling establishment (Hu et al., 2021), and mineral and organic accretion (Foster--Martinez et al., 2023). To assess different restoration strategies, modeling tools, either numerical, physical, or conceptual, are needed to reflect interdependent processes. Consequently, deltaic models require a detailed understanding of these complex interactions, which poses significant challenges for researchers. One of the major challenges in deltaic processes modeling is the large spatial and temporal scales involved (Syvitski et al., 2009; Wasklewicz et al., 2017). Deltas can extend over several thousand square kilometers and undergo changes over decades or even centuries. Another challenge is the complex interactions between physical, biological, and chemical processes that occur in all deltaic systems. Also, deltaic processes can be highly sensitive to human activities, such as dam construction, coastal development, and land-use changes. These activities can alter the natural flow of

* Corresponding author.

E-mail address: akhalfal@tulane.edu (A.M. Khalifa).

<https://doi.org/10.1016/j.ecss.2024.108899>

Received 16 January 2024; Received in revised form 5 July 2024; Accepted 31 July 2024

Available online 31 July 2024

0272-7714/© 2024 The Authors. Published by Elsevier Ltd. This is an open access article under the CC BY license (<http://creativecommons.org/licenses/by/4.0/>).

water and sediment in the river, which can have significant impacts on the deltaic system (Meade and Moody, 2010; Angamuthu et al., 2018). The complex and dynamic nature of deltaic systems means that modeling efforts need to be adaptable and flexible. Models must be able to account for changes in the environment and adjust to new data and understanding as it becomes available. This requires ongoing research and development, as well as collaboration between researchers from different disciplines.

Numerical models are widely used to study coastal and deltaic systems around the globe. They are broadly used for research, planning, and engineering design (Wang et al., 2009, 2014; Stark et al., 2016; Gaweesh and Meselhe, 2016; Meselhe et al., 2016, 2021b; Xing et al., 2017; White et al., 2019a, 2019b; Reed et al., 2020). While models exhibit uncertainties (Meselhe et al., 2021b), they can provide valuable information and insights regarding coastal systems dynamics and their response to the implementation of restoration strategies (Rego et al., 2010). Based on the assumption that ecological processes do not substantially influence the hydrodynamic processes, most studies used a one-way relationship to flow information between physical and ecological models (Collins and Bras, 2004; D'Alpaos et al., 2006; Edmonds and Slingerland, 2007; Yuill et al., 2016). However, to adequately capture the complex ecosystem processes, their feedback must be represented (Meselhe et al., 2015; Baustian et al., 2018; USACE, 2020). For example, the physical presence of vegetation influences the water movement and affects the sediment erosion and deposition processes. Further, submerged and emergent vegetation in wetland regions take up nutrients, their roots grow and consolidate soils, and their stem density changes drag, water circulation, flow velocities, water level, and salinity. Conversely, hydrodynamic parameters such as water depth and salinity influence vegetation composition, and conversion between open water and marshland (Meselhe et al., 2015; Baustian et al., 2018; USACE, 2020). These two-way relationships are important to correctly model the complexity associated within an ecosystem; however, it is challenging to incorporate such feedbacks into the model in a computationally efficient way. Examples of numerical modeling applications to coastal and deltaic systems include Lauzon and Murray (2022) who examined the effect of sediment and flow discharge on synthetic delta building under various conditions of channel stabilization due to vegetation. They found that, compared to those without vegetation, vegetated deltas are muddier, have lower elevations with more stable channels, and steeper water surface slopes. Also, they found that vegetation is able to stabilize the channel network under high discharges of water and sediment by reoccupation of abandoned channels instead of incising new channels or shifting through vegetated regions (Lauzon and Murray, 2022). Kalra et al. (2021) developed a 3D coupled wave-flow-sediment framework that accounts for biomass-produced vertical accretion and erosion of marsh edges due to lateral wave forces. They defined a simplified biomass production technique that compared hydroperiod from tidal datums and marsh elevation. They observed that the marsh interior is dominated by organic deposition where marsh edge is dominated by estuarine mineral deposition (Kalra et al., 2021). Temmerman et al. (2003, 2004) developed a refined zero-dimensional time-stepping model (MARSED) that simulates the variations in tidal marsh sedimentation in response to SLR and changes in suspended sediment concentrations (SSC). They validated their model against field data from 25 vegetated sites in Belgium. This model was able to quantify the combined effect of sea level change and SSC on variations in accumulation rates (Temmerman et al., 2003, 2004). The recently developed version of the same model was able to simulate the interaction between hydrodynamics and vegetation dynamics by calculating the biomass on a 1 m² resolution vegetation grid that is coupled with a several km² resolution hydrodynamic grid for several decades period (Gourgue et al., 2022). Although the biomass calculation responds to morphodynamic change and matches well with observations, the model is not capable of simulating the entire landscape of several hundreds of km² (Gourgue et al., 2022). Reed et al. (2020) used a

lower resolution model for coastal Louisiana to examine the spatial and temporal variability in future wetland loss over thousands of km² and how different factors contribute to the total wetland loss. Reed et al. (2020) showed, using fifty-year model results, that marsh edge erosion is relatively consistent in magnitude across different environmental scenarios, but there was great variation in land loss caused by excessive inundation.

These advances in modeling applications to coastal and deltaic systems, are all limited in how they account for hydrodynamics, morphological change, and vegetation dynamics at a landscape scale. An Integrated Biophysical Model (IBM) was developed and was successfully applied to part of coastal Louisiana (Meselhe et al., 2015; Baustian et al., 2018; USACE, 2020). The IBM was used to perform long term (decadal) landscape evolution simulations, assess responses of deltaic and coastal systems to climate change scenarios, and inform ecosystem restoration strategies. The IBM attempted to account for some two-way relationships as it modeled dynamic coupling among (1) morphodynamics, (2) nutrient dynamics, (3) hydrodynamics, and (4) vegetation dynamics. More details about the internal dynamics regarding the coupling are outlined in detail in previous studies (Meselhe et al., 2015; Baustian et al., 2018; USACE, 2020). Although the IBM is a highly detailed biophysical model (Baustian et al., 2018), it exhibits two main drawbacks: (1) the model needs 24–48 h to complete a single year run, and (2) often, the calculated accretion rates from the biomass processes are lower or higher than the range depicted from field observations (Baustian et al., 2023). Thus, the calculated accretion rates had to be controlled by values from the field observations for each vegetation species. These two limitations were the impetus for developing a simplified modeling approach to significantly reduce the computational burden and capture, to the extent possible, the two-way interaction among the hydro, morphology, and vegetation dynamics.

In this study, hydrodynamic and morphodynamic Delft3D models are coupled with a new developed MATLAB script that captures the effect of marsh inundation on accretion rates and consequently on the landscape evolution. This newly developed model, the Simplified Biophysical Model (SBM), is simpler than the previous detailed IBM (Baustian et al., 2018), as it does not explicitly model vegetation or nutrient dynamics and it does not have detailed two-way relationship between hydrodynamic and morphodynamic components. However, it is substantially more computationally efficient (10 times faster) to perform decadal morphodynamic and landscape evolution simulations. The computational efficiency is highly beneficial as it allows performance of a large number of scenarios to examine variety of climate change conditions or a range of restoration strategies with a reasonable simulation time (days) (Meselhe et al., 2022; Khalifa, 2023).

This paper describes the model approach and structure and the results of calibration and validation over a hindcast period (1994–2020) where modeled land loss trends are compared with land loss estimates from aerial imageries (Couvillion, 2017; Couvillion et al., 2017) for two estuarine Basins in Louisiana. To demonstrate its utility, the paper presents results from application of the SBM to assess the land building potential and performance of the proposed Mid-Barataria Sediment Diversion (MBSD), and impact of sediment load reduction in the Mississippi River Delta (MRD) on the potential land building from the MBSD.

2. Data and methods

2.1. Model development

The primary components of the SBM are: (1) hydrodynamic model, (2) morphodynamic model, and (3) marsh inundation module. There is interaction and feedback among these three components during decadal simulations as shown in Fig. 1. Each of the three components is described in the following subsections. More details are presented by Khalifa (2023).

Simplified Biophysical Model (SBM)

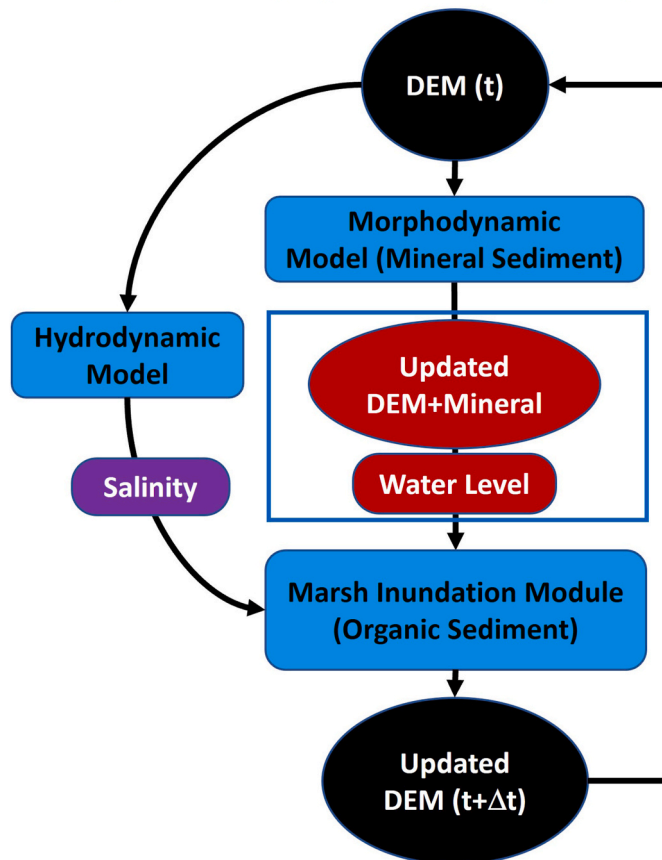


Fig. 1. SBM schematic diagram. Blue polygons represent the three different components utilized through the SBM as: (1) hydrodynamic model, (2) morphodynamic model, and (3) marsh inundation module. Revised from Khalifa (2023). (For interpretation of the references to color in this figure legend, the reader is referred to the Web version of this article.)

2.1.1. Hydrodynamic model

The open source physical processes based numerical model Delft3D (V-6.04) modeling suite (Lesser et al., 2004) developed by Deltares (<http://www.deltares.nl/en/>), which has been used widely for hydrodynamic studies (Elias et al., 2001; Luijendijk, 2001; Baustian et al., 2018; Ramakrishnan et al., 2019; Thanh, 2021; Hu et al., 2022), was selected to provide the hydrodynamic calculations for the SBM. Delft3D-FLOW is a multidimensional hydrodynamic model that calculates non-steady flow that results from tidal, source-sink and meteorological forcing on a curvilinear or boundary-fitted grid. It solves the Navier Stokes equations for incompressible fluid, under the three-dimensional or depth averaged shallow water and the Boussinesq assumptions (Lesser et al., 2004). More information about Delft3D-FLOW can be found in <https://content.oss.deltares.nl/delft3d/manuals>. A set of full hydrodynamic annual simulations are performed independently to obtain annual averaged salinity at every computational point in the model domain. Spatially varied subsidence is added to the initial digital elevation model (DEM) on an annual basis. Each year, the annual averaged salinity map is passed to the third component of the SBM (marsh inundation module) to be used for organic accretion calculations.

2.1.2. Morphodynamic model

The SBM utilizes the open source morphodynamic numerical model Delft3D (Lesser et al., 2004) suite developed by Deltares (<http://www.deltares.nl/en/>) to simulate mineral sediment transport. This model

has been used widely for both conceptualization and morphodynamic case studies in coastal and riverine environments (Elias, 1999; Caldwell and Edmonds, 2014; Reyns et al., 2014; Sandén et al., 2016; Yuill et al., 2016; Gaweesh and Meselhe, 2016; Meselhe et al., 2016, 2021a; Baustian et al., 2018; Brakenhoff et al., 2020; Morgan et al., 2020). It has the capability to calculate the sediment flux for coarse/non-cohesive sediment fractions in riverine environments through a variety of available sediment transport equations (e.g., Meyer-Peter-Muller, 1948; Engelund-Hansen, 1967; Ashida-Michiue, 1974; Van Rijn, 1984; Wilcock-Crowe, 2003). Additionally, it uses different sets of equations to simulate coastal environments (e.g., Bijker, 1971; Van Rijn, 1993; Soulsby, 1997; Van Rijn, 2003; Van Rijn, 2007). In contrast, it calculates sediment fluxes for fine/cohesive sediment fractions through one equation: Partheniades (1965). The SBM uses Van Rijn (2007); Van Rijn (2007); Partheniades (1965); Partheniades (1965) equations to calculate the sediment fluxes from non-cohesive, and cohesive sediment fractions, respectively. More information about Delft3D sediment transport equations, can be found in <https://content.oss.deltares.nl/delft3d/manuals>. On annual basis, the SBM uses this morphodynamic model to update the initial DEM and passes the new updated DEM (Updated DEM + Mineral in Fig. 1), and annual averaged water level (WL) to the third component (marsh inundation module) to be used for organic accretion calculations. The DEM annual updating interval is selected primarily because the available relationships between salinity and marsh inundation tolerance are based on annual averages. Further, the available information about accretion rates is also annual. Thus, there will be no justification to increase the frequency of update to the DEM other than the interaction between hydrodynamics and morphodynamics. If more frequent data are available, the model is capable of adjusting the updating interval. However, given that we are using morphological acceleration, we do not believe any benefit would be realized from updating the DEM update frequency.

2.1.3. Marsh inundation module

A marsh inundation module was developed using MATLAB programming language as shown in Fig. 2. This module consists of three main steps described by the numbers 1 to 3 in the figure.

In the first step the pre-generated annual averaged salinity map obtained from the hydrodynamic model is used to create a marsh type classification map based on salinity weighted average score as described by Baustian et al. (2023) and listed in the supplement material. The salinity map is used to drive a calculation of an annual inundation depth (D_i). The D_i map represents the maximum submergence depth that vegetation can tolerate. This approach is based on the Integrated Compartment Model (ICM) used for the 2023 Louisiana Coastal Master Plan (CMP) (Baustian et al., 2023; Foster-Martinez et al., 2023). This approach relies on data from the Coastwide Reference Monitoring System (CRMS) that identifies a relationship between salinity and annual average water depth tolerated by vegetation.

In the second step the water depth (D) and D_i are used together to classify each cell into marsh or water. A model cell is classified as marsh if D is lower than D_i and water if D is larger than D_i . Marsh cells produce organic material based on marsh type (assigned in the first step), while water cells do not.

In the third step the subsequent year's calculation determines whether a marsh cell will sustain its classification or if it would convert to water. For a given cell, where the depth (D) exceeds the maximum inundation depth (D_i -guided by salinity) for two consecutive years, it would convert to water. Water cells can convert into marsh, based on the emergence depth (D_E) value, and start producing organic accretion or remain as water. Water cells convert to marsh if the annual averaged water depth is lower than or equal to emergence depth (D_E) that is considered 0.1 m in this study (Foster-Martinez et al., 2023). D_E represents the water depth threshold for new vegetation establishment. Organic accretion rates applied to marsh cells vary with marsh types and are based on measurements in coastal Louisiana as shown in Table 1

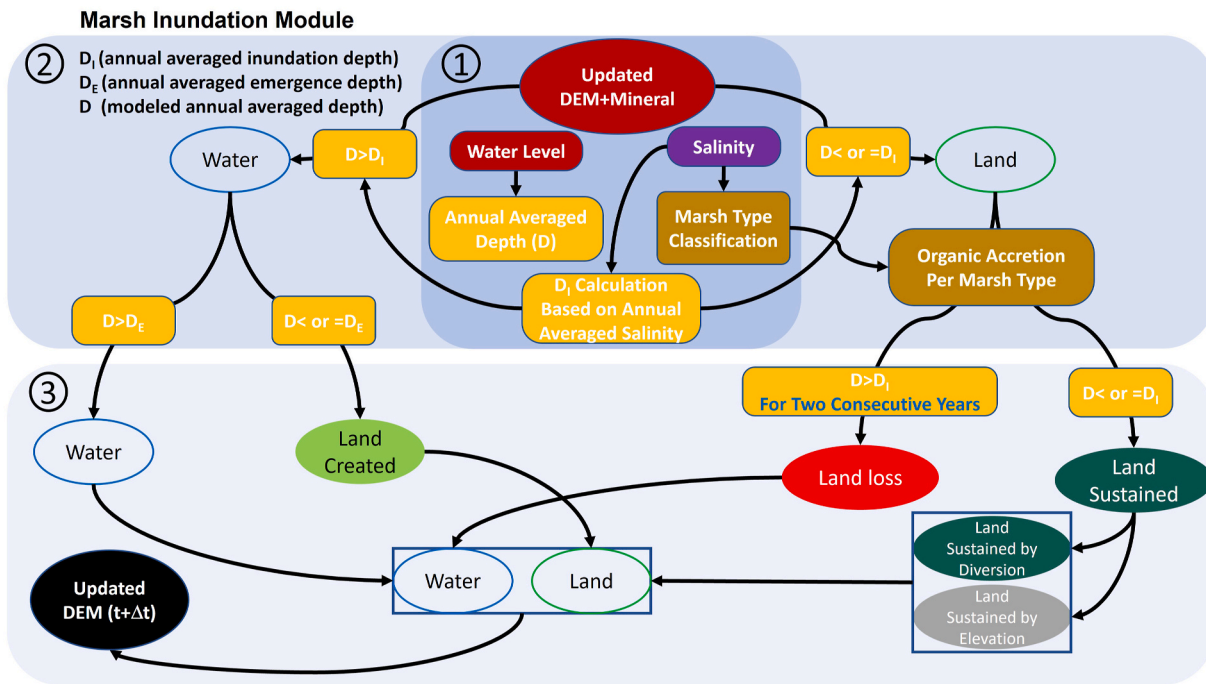


Fig. 2. Marsh inundation module. (D_i) is the maximum annual averaged inundation depth that vegetation can tolerate, (D_E) is the annual averaged emergence depth, and (D) is the modeled annual averaged depth. Purple polygon represents data obtained from the hydrodynamic model. Maroon polygons represent data obtained from the morphodynamic model. Dark brown boxes represent calculations depending on marsh type. Orange boxes represent water depth comparisons. Different oval shapes' colors represent different land categories where red is land loss, light green is land created, dark green is land sustained due to a restoration strategy (if applicable), and grey means land sustained due to the bed elevation. (For interpretation of the references to color in this figure legend, the reader is referred to the Web version of this article.)

Table 1
Organic accretion rates for the Barataria Basin including limits used in model calibration revised from Baustian et al. (2023).

Marsh Type	Lower Limit-2SD Barataria rates (mm/yr)	Lower Limit-1SD Barataria rates (mm/yr)	Median Limit Barataria rates (mm/yr)	Upper Limit Barataria rates (mm/yr)	CMP2023 Coast Wide rates (mm/yr)
Fresh	7.50	9.61	11.71	14.08	11.70
Intermediate	7.89	8.95	10.00	11.18	8.20
Brackish	6.71	7.63	8.55	9.74	8.30
Saline	7.63	9.21	10.79	12.76	12.20

(Baustian et al., 2023).

The module produces, annually, an updated DEM (Updated DEM-(t + Dt)) based on the calculated organic accretion rates. This updated DEM is fed into the morphodynamic model for mineral sediment calculations of the following year. Through this process, the SBM accounts for the interaction between landscape morphology and marsh inundation induced by changes to the water and salinity due to SLR, restoration strategies, etc. as shown in Fig. 2. The typical run time for the SBM is ~0.8, 2.5, and 4.7 days real time for one, three, and five decade simulations for an area of 4500 km² defined by 295,400 nodes.

2.2. Modeling the lower Mississippi River's adjacent Basins

The MRD in coastal Louisiana, USA is utilized here as a case study (Fig. 3). This delta and the adjacent estuaries are subjected to high RSLR rates, up to 20 mm/year (Byrnes et al., 2019). Based on 66 tide gauge records from the Permanent Service for Mean Sea Level (PSMSL) along the North American and Gulf coast and covering the period 1900–2021, Dangendorf et al. (2023) showed peak-to-peak variations in Mean Sea Level (MSL) of ~45 mm (~25 mm due to open ocean wind stress forcing

with additional contributions from coastal longshore winds and river discharge) on multi-year timescales such internal variability may either mask or amplify externally forced trends and acceleration along this coastline. Construction of dams along major Mississippi River (MR) tributaries reduced the sediment supply and increased the likelihood of drowning of the MRD coastal wetland system due to RSLR (Allison and Meselhe, 2010). Similarly, leveeing the MR has cut the connection between the river and its floodplains that consequently controlled river meandering and reduced the sediment supply (Allison et al., 2012) to adjacent wetlands. Canals dredged across the coast alter hydrology leading to loss of coastal wetlands and progradation of wave forces further upland into the coastal regions (Scaife et al., 1983). Although, hurricanes nourish the MRD with mineral sediments from offshore and onshore sources, they generate storm surge that can cause erosion in vegetated and unvegetated areas (Palaseanu-Lovejoy et al., 2013; Bevington et al., 2017). These and other modifications to the system result in land loss – conversion of wetlands to open water.

The focus here is to examine the loss of coastal Louisiana wetlands due to: (1) the lack of mineral deposition that used to nourish the delta and (2) RSLR. These two combined impacts change the relative elevation of a marsh in the tidal frame and can result in larger inundation depth, higher inundation duration, higher inundation frequency, and ultimately marsh collapse and land loss (Couvillion and Beck, 2013; Couvillion, 2017; Couvillion et al., 2017). Thus, as the main focus for restoration is to retain remaining wetlands in coastal Louisiana and restore the deltaic processes to build additional wetlands (CPRA, 2023), our analysis will consider temporal and spatial landscape response due to changes in marsh elevation resulting from changes in mineral sediment input and RSLR including the influence of organic accretion.

2.2.1. Model setup

A previously developed 3D hydrodynamic and salinity model with seven sigma layers has been used to calculate salinity patterns in Barataria and Breton Sound Basins as shown in Fig. 3 (Hu et al., 2022,

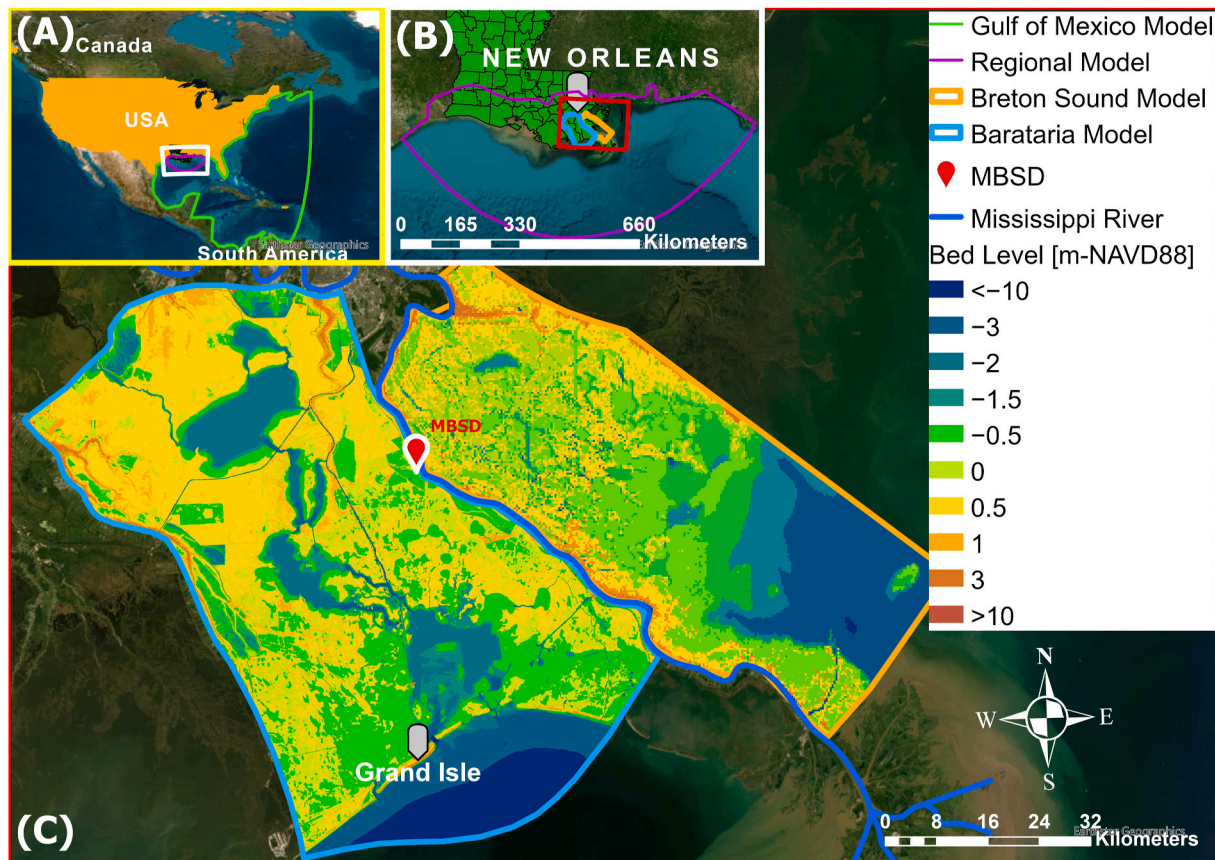


Fig. 3. Barataria and Breton Sound Basins, and different hydrodynamic nested layers' domains. (A) Location of Louisiana and the extent of the regional hydrodynamic model within the Gulf of Mexico model domain. (B) Location of Barataria and Breton Sound Basins and the extent of the two local models within the regional domain. (C) DEM data in (m-vertically referenced to North American Vertical Datum NAVD-88). The location of the proposed Mid-Barataria Sediment Diversion (MBSD) is indicated by the red mark. (For interpretation of the references to color in this figure legend, the reader is referred to the Web version of this article.)

2023). Three computational domains were set up for nesting (Hu et al., 2015, 2022, 2023) computation as: (1) Gulf of Mexico model, (2) regional model, and (3) local model as shown in Fig. 3. The Gulf of Mexico model covers the entire Gulf of Mexico and part of the Atlantic Ocean with a spatial resolution ranging from 6 km near Louisiana coast to 40 km in the Atlantic Ocean. From a tidal constituent database (Mukai et al., 2002), seven dominant constituents (O1, K1, Q1, M2, N2, S2 and K2) are considered to determine tidal levels at the open-sea boundary across the Atlantic Ocean. The purpose of this large-domain model is to provide water level boundaries for the regional model (Hu et al., 2023). The second coupled layer (regional model) focuses on Louisiana coast in the north-central region of the Gulf of Mexico (Hu et al., 2023). The MR discharge data are either from gauge observations (if available) or estimates from the 2017 CMP model input (Hu et al., 2023). The third coupled layer (local model) encompasses the main part of Barataria Basin or Breton Sound Basin. More details on the development of this hydrodynamic model is available by Hu et al. (2023). The simulated local domain is subsided from year to year based on a predefined subsidence map assuming constant rates through years. Also, the hydrodynamic model accounts for SLR variations.

The two local models described in the previous paragraph have fine grid size ranges from 50 m to ~200 m. The USGS 5 m-resolution National Elevation Dataset (<http://ned.usgs.gov/>) is used as the primary source of the topo-bathymetric of the local models. The two morphodynamic local models presented here are parameterized based on previous modeling efforts for the same and neighboring Basins (Allison et al., 2017; Baustian et al., 2018; Meselhe et al., 2015, 2021a; Sendorowski et al., 2018; Yuill et al., 2016). These previous modeling efforts

detailed the validated model outputs against field observations. A summary of the model parameters used here include horizontal eddy viscosity and diffusivity of 2 and 20 $\text{m}^2 \text{s}^{-1}$, respectively. Five sediment fractions (sand, silt, clay, consolidated clay, and marsh soil) where consolidated clay and marsh soil are used to define the initial Basin substrate and sand, silt, and clay are used to define the diverted loads from the MR through restoration strategies (if applicable) (Baustian et al., 2018). Spatially variable Chezy roughness is used ranging from 60 (land) to 75 (open water and channels) (Meselhe et al., 2022). Based on a sensitivity analysis along with guidance from the previous modeling efforts (Meselhe et al., 2015, 2022; Baustian et al., 2018; USACE, 2020), the morphological simulation was accelerated using a morphological acceleration factor (MorFac) of 80 to reduce the simulation time (Roelvink, 2006). The substrate was designed with total of 30 layers covering a 20 m depth where the top 1 m is surficial uncompacted fine sediment layer and the bottom 19 m are consolidated clay (Bomer et al., 2019). The top 15 layers have 0.3 m thickness while the bottom 15 layers have 1-m thickness each. More details on the morphodynamic model design and calibration are presented in Khalifa (2023). The morphodynamic model boundaries include an offshore open boundary to reflect SLR rates.

2.2.2. Model validation

2.2.2.1. Hydrodynamic model calibration and validation.

The year of 2018 is selected for the hydrodynamic model calibration and validation following previous studies (Hu et al., 2022, 2023). Daily water level, and salinity data are collected at CRMS and United States Geological Survey

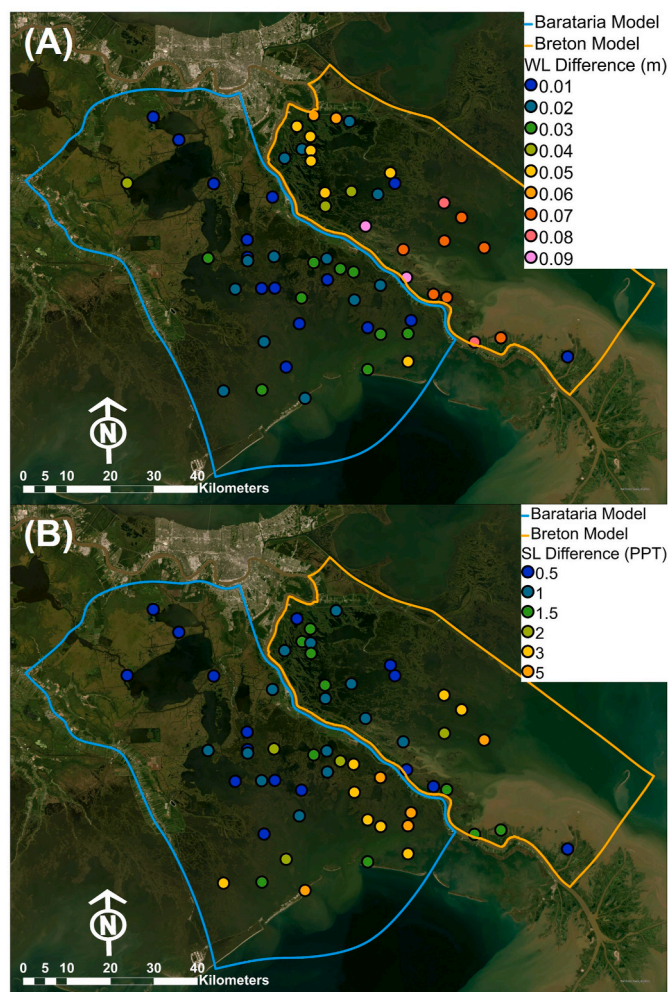


Fig. 5. Barataria and Breton Sound hydrodynamic models' validation. (A) Difference between modeled and observed annual averaged WL at different stations. (B) Difference between modeled and observed annual averaged salinity at different stations.

calibration period (1994), the 2020 DEM is used as is, and landscape evolution comparison is done using the land loss trend rather than absolute values as shown in Fig. 6. All sensitivity runs' results are represented in the grey envelope shown in Fig. 6-A. The modeled landscape evolution shows a good response to the environmental drivers and a reasonable comparison to the historical landscape evolution trend. Run #20 shows a reasonable agreement between the historical and modeled estimates and thus concluded as a calibrated setup. The same set of parameters used in the calibration effort in Barataria is used to validate the SBM for Breton Sound. Landscape areas' estimates (Couvillion, 2017; Couvillion et al., 2017) are used to assess the modeled landscape evolution. Fig. 9-B shows a good agreement between the modeled land loss trend and the historical estimates. Through the sensitivity analysis, subsidence is defined as a primary driver that shows the highest impact on the modeled land loss. This agrees with the findings from Edmonds et al. (2023) where resources extraction that influences deep subsidence is defined as the most important cause for land loss in Barataria Basin. Run 11 and Run 23 have subsidence ranges of (3.6–8.8), and (6–13) mm/years, and they correspond to the highest and lowest limits that define the grey shade in Fig. 6-A, respectively. A 65-45% increase in subsidence corresponds to an excessive land loss of 54, 94, and 226 Km² by 2000, 2010, and 2020, respectively as shown in Figure S 11-A in the Supplement Material. The second important sensitivity parameter is the annual accretion rate where a 2 standard deviation change in the

Table 2

Calibration runs attributes. Run ID with (*) shape represent runs with better fit to the calibration dataset.

Run-ID	Organic Accretion Rates	Subsidence	Emergence Depth (D _E) for Existing Marsh (m)
1	2023 CMP (Mean)	CMP 2017 (3.6–8.8) mm/year	0
2	2023 CMP (Mean)	CMP 2017 (3.6–8.8) mm/year	0.1
3	2023 CMP (Mean)	CMP 2017 (3.6–8.8) mm/year	0.2
4	2023 CMP (Mean)	CMP 2017 (4–9.5) mm/year	0.1
5	5 mm	CMP 2017 (3.6–8.8) mm/year	0
6	5 mm	CMP 2017 (3.6–8.8) mm/year	0.1
7	5 mm	CMP 2017 (3.6–8.8) mm/year	0.2
11*	Lower Limit 2023 CMP (Barataria)	CMP 2017 (3.6–8.8) mm/year	0.1
12	Median Limit 2023 CMP (Barataria)	CMP 2017 (3.6–8.8) mm/year	0.1
13	Upper Limit 2023 CMP (Barataria)	CMP 2017 (3.6–8.8) mm/year	0.1
14	Lower Limit 2023 CMP (Barataria)	CMP 2017 (3.6–8.8) mm/year	0.2
15	Median Limit 2023 CMP (Barataria)	CMP 2017 (3.6–8.8) mm/year	0.2
16	Upper Limit 2023 CMP (Barataria)	CMP 2017 (3.6–8.8) mm/year	0.2
17*	Lower Limit 2023 CMP (Barataria-2SD)	CMP 2017 (3.6–8.8) mm/year	0.1
18*	Lower Limit 2023 CMP (Barataria)	CMP 2017 (4–9.5) mm/year	0.1
19*	Lower Limit 2023 CMP (Barataria-2SD)	CMP 2017 (4–9.5) mm/year	0.1
20*	Lower Limit 2023 CMP (Barataria)	CMP 2017 (4.4–10.2) mm/year	0.1
21*	Lower Limit 2023 CMP (Barataria)	CMP 2017 (5.5–11.6) mm/year	0.1
22*	Lower Limit 2023 CMP (Barataria)	CMP 2017 (5.6–12.3) mm/year	0.1
23*	Lower Limit 2023 CMP (Barataria)	CMP 2017 (6–13) mm/year	0.1

accretion rate corresponds to excessive land loss of 12, 20, and 57 Km² by 2000, 2010, and 2020, respectively as shown in Figure S 11-B in the Supplement Material. The third and least effective sensitivity parameter is the emergence depth (D_E). A decrease in D_E from 0.2 m to 0 m corresponds to an excessive land loss of 9, 12, and 55 Km² by 2000, 2010, and 2020, respectively as shown in Figure S 11-C in the Supplement Material.

3.2. Restoration strategy: sediment diversion

3.2.1. Environmental drivers and implementation dates

To date, coastal restoration planning in Louisiana's coast has been based on projected SLR scenarios laid out in the Coastal Master Plans (CPRA, 2023) and the goal of restoration planning in Louisiana has been to slow down land loss in a sediment-starved coastal system. One of the common restoration strategies targeted in the Louisiana Coastal Master Plan (CPRA, 2023) is sustaining and rebuilding wetlands through mimicking a natural deltaic formation process using sediment diversions from the river. The MBSD is one of the proposed sediment diversions (Meselhe et al., 2016, 2022; CPRA, 2017, 2023) and is utilized here as an example application to show the SBM applicability to existing deltaic systems. It will be located on the west bank of the MR in Barataria Basin as shown in Fig. 3.

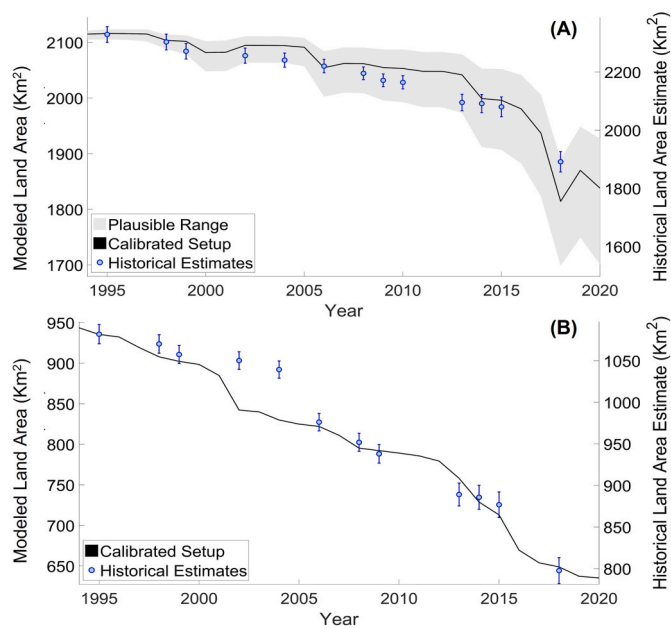


Fig. 6. Relative land loss calculated by the SBM are shown in the left Y-axis and the absolute historical land estimates are represented on the right Y-axis (Couvillion, 2017; Couvillion et al., 2017). Panel (A) is for Barataria where the grey shade represents the range of land loss estimates from all the sensitivity runs. The black line shows land loss trend from the calibrated setup (Run #20). Panel (B) is for Breton Sound. Uncertainty of the historical land estimates (Couvillion et al., 2017) is presented as whiskers for one higher and one lower standard error. (For interpretation of the references to color in this figure legend, the reader is referred to the Web version of this article.)

Meselhe et al. (2022) used an extensive set of numerical experiments to examine the impact of key environmental drivers on the performance of the MBSD used as a coastal restoration strategy. They considered different environmental drivers as:

- Land subsidence. Two spatially variable subsidence maps were used based on Reed and Yuill (2017) and Byrnes et al. (2019). These subsidence rates were assumed to persist over the simulation duration. Incorporating subsidence into models is challenging due to the complexity of the process (shallow versus deep subsidence), limited understanding of how these processes vary with time, and its strong spatial heterogeneity (Dokka et al., 2006; Yuill et al., 2009). In Louisiana, USA, a panel of experts (guided by some field observations) developed spatially variable subsidence ranges for use in the 2012 and 2017 CMP (Shinkle and Dokka, 2004; Reed and Yuill, 2017). The plan used 20% (3.6–8.8 mm/year) and 50% (6–13 mm/year) of the identified range to represent moderate and high scenarios, respectively. Observations that report historical declining rates of subsidence from Shinkle and Dokka (2004) supported that assumption and suggested that in the next 50 years, subsidence rates will be within the lower end of the range (Reed and Yuill, 2017). For the SBM, we adopted the approach presented by Reed and Yuill (2017), however, these rates can be adjusted for applications to other coastal or deltaic systems.
- SLR rates. Incorporating the eustatic component is fairly a straightforward process once a specific curve is selected. Two SLR rates with a projected elevation of 1 m and 2 m by 2100 were assumed for consistency with values used in the Louisiana Coastal Master Plan (Meselhe et al., 2022).
- Mississippi River inflow hydrographs. Five riverine hydrographs, including four climate scenarios and one historical record were selected. These climate scenarios are based on the Coupled Model Intercomparison Project phase 5 (CMIP5) projections span from

1950 through 2100 (Lewis et al., 2019). The Routing Application Parallel Discharge (RAPID (David et al., 2011; Tavakoly et al., 2017),) numerical model was used to route runoff datasets provided by executions of the Variable Infiltration Capacity (VIC (Liang et al., 1994),) hydrologic model. The VIC model has been executed with its boundary conditions provided by the downscaled and bias corrected global climate models. Daily streamflow was generated for the entire Mississippi River Basin (MRB) at more than 1.2 million river reaches using high performance computer (HPC) systems.

- Sediment rating curves. To estimate the mineral sediment loading in the MR, two sediment rating curves were used. The first rating curve, namely USGS is based on previous studies (Allison et al., 2012; Meselhe et al., 2016) while the second rating curve estimates the hysteresis effects (Peyronnin et al., 2017). More details and comparisons are available in the Supplement Material.
- MBSD operation date. They considered MBSD hypothesized operation date of 2025, 2030, and 2035 for the MBSD.

To demonstrate the utility of the SBM for helping decision makers explore the implications of different assumptions about future conditions, a subset of five scenarios from the full 240 morphodynamic runs presented in Meselhe et al. (2022), are selected. The five selected scenarios represent the 10th, 25th, 50th, 75th and, 90th percentiles of the land change envelope of possibilities derived from the 240 morphodynamic runs conducted in the previous study (Meselhe et al., 2022). These scenarios are modeled using the SBM to demonstrate its ability to produce decadal landscape changes in a computationally efficient manner. The selected scenarios and corresponding attributes are presented in Table 3. It should be noted that the five scenarios are simulated with and without the MBSD to isolate the positive and negative impacts of the MBSD. Decadal results from the IBM are extracted and compared to the annual potential land building and land change from the SBM. The attributes of the IBM two environmental scenarios are shown in Table 3.

The results of the five representative scenarios were analyzed and corresponding net land change was calculated by subtracting remaining land from scenarios with and without the MBSD as shown in Fig. 7-A. Fig. 7-B shows the remaining land percentage for each scenario with and without the MBSD compared to the existing landscape in 2020. The two landscape change maps at year 2099 presented in Fig. 8 show: (A) 10th percentile (lowest net land change) and (B) 90th percentile (highest net land change).

3.2.2. Sustained and declining sediment loads

Kleiss et al. (2021) generated trends for different water quality parameters from different USGS stations along the MR path where SSC showed a declining trend from 1997 to 2019, typically at an annual rate of around -1.5% (Mize et al., 2018; Kleiss et al., 2021). This loss in SSC could be influenced by possible deposition of fine sediments on top of the flood plain and other sinks along the river. Similarly, Mossa (1996) reported an overall decline in average annual suspended sediment load of 70% since 1850. Declining trend that started in 1930 was associated with soil conservation policies and erosion control measures that include contour plowing, trees and plants on denuded landscapes replanting and, constructing small sediment retention dams, and stabilizing banks. During 1950–1980, most sediment decline is associated with construction of dams on the Missouri River. Studies of historical changes suggest that in suspension sand amount and bed material size decreased during the same period (Mossa, 1996; Meade and Moody, 2010).

In order to examine the impact of the MR sediment supply decline on potential land building from the MBSD, two annual declining sediment rates are considered: -1.5% (Kleiss et al., 2021) and -3% (Rebich and Demcheck, 2007; Meade and Moody, 2010). The impact of annual sediment decline rates on calculated suspended sand and fines is shown in the Supplement Material. The 90th and 50th scenarios are rerun with sediment declining rates yielding a total of four new scenarios: 90th with 1.5% decline, 90th with 3% decline, 50th with 1.5% decline, and 50th

Table 3
Attributes of the environmental driver scenarios.

Scenario-ID	MR Hydrograph	SLR (m) By 2100	Sediment Rating	Construction Date
10 Percentile	miroc5-rcp45 (10)	2	Hysteresis	2035
25 Percentile	miroc5-rcp45 (10)	1	USGS	2035
50 Percentile	miroc5-rcp45 (10)	1	Hysteresis	2035
75 Percentile	bcccsml1m-rcp45 (1)	1	USGS	2025
90 Percentile	bcccsml1m-rcp45 (1)	1	Hysteresis	2025
IBM (low)	Historical record	0.79	Hysteresis	2020
IBM (high)	Historical record	1.5	Hysteresis	2020

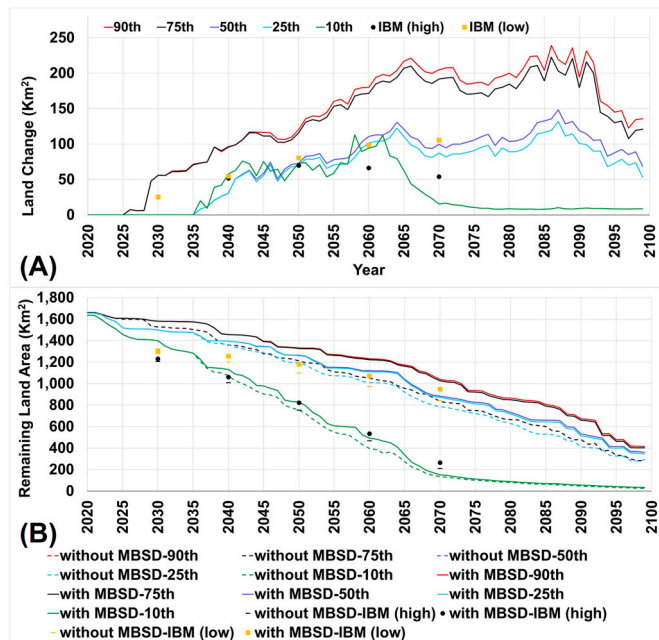


Fig. 7. (A) Land change for different scenarios calculated as the difference between the remaining marsh from each scenario with MBS and the corresponding scenario without MBS. (B) Remaining land area for different scenarios for both scenarios with and without MBS.

with 3% decline. Fig. 9 shows the negative impact of the two sediment decline rates on the potential land building from the MBS compared to the no decline assumption.

4. Discussion

4.1. Verification of the simplified biophysical model applicability

To conserve computational resources, we use 2D local models to represent the two Basins instead of 3D local models. While there is no significant salinity stratification inside the Basin, a 3D regional model is essential to establish the open water boundary for the local model. This approach is presented in Hu et al. (2023). A full analysis was performed to assess the performance of 2D versus 3D modeling of both regional and local domains. The analysis showed the importance of running the regional model in a 3D mode to establish reasonable boundaries to the local 2D domain. Using 2D for the local domain was adequate as long as it is driven by a regional 3D model. In addition, based on the salinity output from the hydrodynamic model, a vegetation distribution map is generated for Barataria Basin for 2013 which is compared to the USGS published vegetation distribution developed from remote sensing and field observations as shown in the Supplement Material. This comparison demonstrates the capability of the SBM inundation module to capture reasonable vegetation distribution. More details on the hydrodynamic model development are described by Hu et al. (2023).

The model results in this study are compared to land building results produced by the previously developed IBM (Meselhe et al., 2015; Baustian et al., 2018; USACE, 2020). Fig. 7 shows a comparison of remaining land and land change, the subtraction of remaining land from without-MBS and with MBS scenarios. The land change comparison isolates the impact of the MBS and its annual potential land building. The land change comparison shows good agreement between the outputs from the SBM and IBM models regarding the magnitude of land building potential. However, the two models utilize two different approaches for organic accretion rates. Also, accretion rates calculated by IBM using LaVegMod (Visser and Duke-Sylvester, 2017) are different from the annual accretion rates utilized in this study for the SBM which are based on recent CRMS measurements (Baustian et al., 2023). These discrepancies in accretion rates from the two models affect both scenarios with and without MBS. In addition, the starting DEM and model domain are not exactly equivalent between the two models. The difference in starting DEM of 2020 and model domain between the two models is shown in Fig. 7-B. There are other differences in environmental forcing assumption between the two models where IBM considers MBS diversion start date in 2020 whereas, the SBM considers updated diversion start date scenarios as 2025 and 2035. Additionally, the SLR scenarios utilized in the IBM runs are 0.79 m and 1.5 m by 2100 whereas, the SBM runs use 1 m and 2 m by 2100 (Table 3). Subsidence rates are also different between the two models where the IBM run uses the rates developed for the 2017 CMP (Reed and Yuill, 2017) and the SBM run uses the recently published rates which are higher (Jankowski and Reed, 2021). Finally, the IBM run uses measured historical MR hydrograph from 1970 to 2020 whereas, the SBM run uses two MR hydrographs generated from the RAPID and VIC climate models (Liang et al., 1994; David et al., 2011; Tavakoly et al., 2017) to represent most severe drought and wet scenarios. The IBM results are reported each decade (USACE, 2020) whereas, SBM has annual results for both land change and remaining land areas. Collectively these differences make comparison of exact land building potential numbers from the two models difficult. However, the bracket of IBM outputs lies within the SBM outputs bracket and within the same magnitude of land building potential (see Fig. 7-A). This shows that, although there are differences between the two model setups, the two studies include similar considerations for which parameters were necessary as model drivers and both models yielded results indicating similar trends in land change response to diversion operation. Specifically, the IBM high SLR scenario (1.5 m by 2100) shows a strong remaining land areas agreement with SBM 10th percentile scenario (2 m by 2100) as shown in Fig. 7-B which emphasizes the high impact of SLR on the outputs from both models and to Barataria ecosystem in general. It should be noted that the SBM is approximately one order of magnitude faster computationally compared to the IBM, which was one of the driving impetus of developing the SBM.

4.2. Sediment diversion potential land building

The two SLR rates used in the analysis produced distinct net land change outcomes. As concluded by Meselhe et al. (2022), SLR and operation date are the most two important parameters that distinguish whether the subdelta formed by the MBS operation remains or diminishes. By 2070, because of the 2 m SLR and the delayed MBS

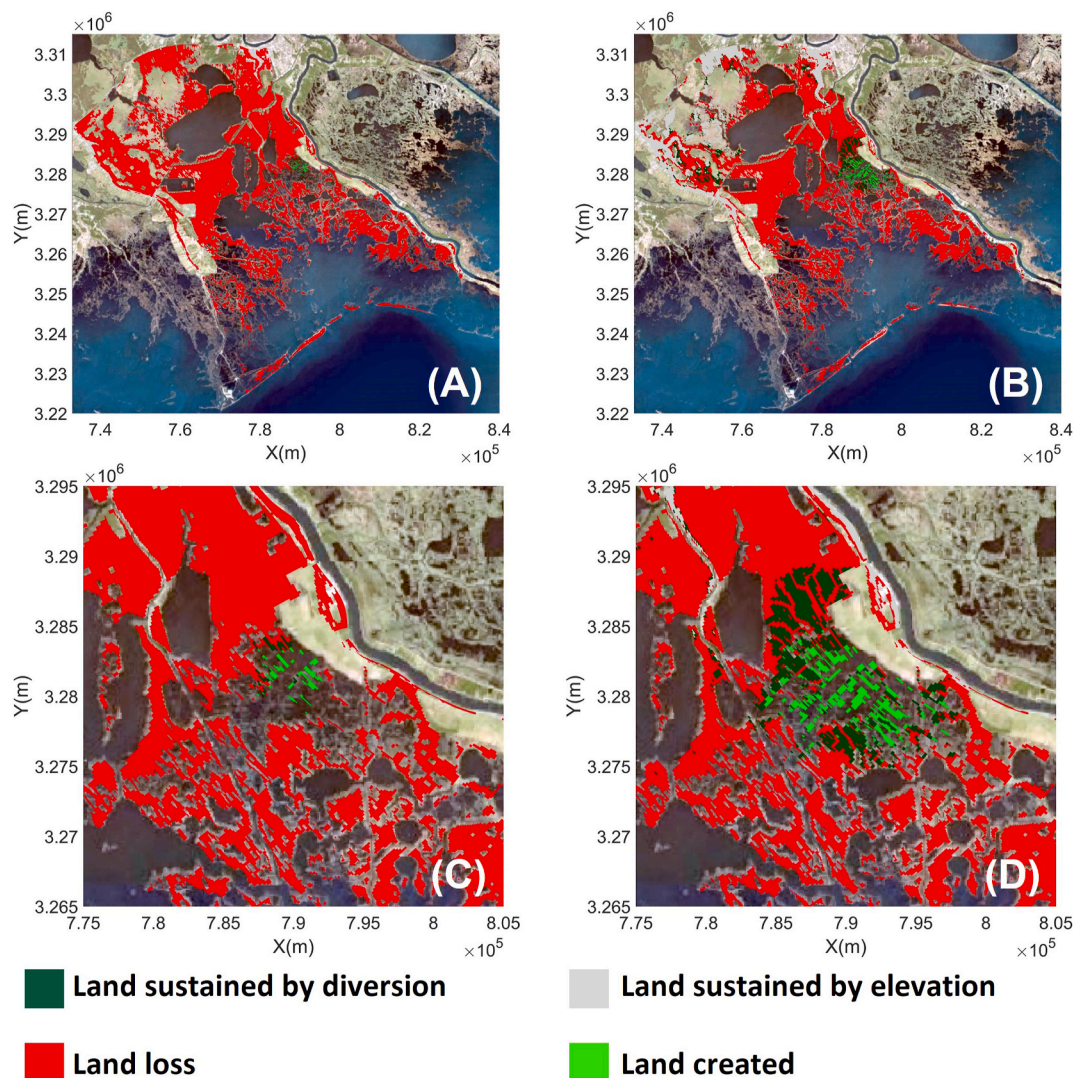


Fig. 8. Net land change map for Barataria Basin by 2099. (A) 10th percentile scenario with the following attributes: Mississippi hydrograph: miroc5-rcp45 (Lewis et al., 2019), SLR 2-m, sediment rating curve: Hysteresis, and operation date of 2035. (B) 90th percentile scenario with the following attributes: Mississippi hydrograph: bccsm11m-rcp45, SLR 1-m, sediment rating curve: Hysteresis, and operation date of 2025. (C), and (D) are similar to (A), and (B), respectively with zoomed in view to focus on the MBSD outfall area. Red represents pixels that started as marsh in 2020 and converted to water by 2099 with or without the MBSD, where grey are pixels that started as marsh in 2020 and remained as marsh by 2099 with or without the MBSD. The dark green represents pixels that started as marsh in 2020 and converted to water by 2099 without the MBSD but was sustained as marsh only due to the presence of the MBSD. The light green represents pixels that started as open water in 2020 and remained water without the MBSD but converted to marsh due the presence of the MBSD. (For interpretation of the references to color in this figure legend, the reader is referred to the Web version of this article.)

implementation date (2035), the 10th percentile scenario shows almost zero land change as the whole Basin has converted to open water. So, both future with and without MBSD show a diminished landscape and almost zero land change. This is indicated in Fig. 7 by the green lines and Fig. 8-A. Establishing a vegetated surface, as early as possible in the simulation significantly increases the annual elevation gain due to the organic accretion ameliorating the influence of SLR and subsidence. The difference between the utilized Hysteresis and USGS rating curves is reflected on the resulted landscape from the 90th and 75th scenarios indicated by the red, and black lines in Fig. 7, respectively. Similar difference is reflected on the resulted landscape from the 50th and 25th scenarios indicated by the blue, and cyan lines in Fig. 7, respectively. Comparing the two utilized rating curves, the Hysteresis rating curve calculated higher suspended sediment and higher sediment loads diverted through the MBSD and thus the modeled landscape shows higher land change indicated by the red line in Fig. 7. Decadal land change maps are presented in the Supplement Material.

4.3. Declining sediment loading

By 2100, the 1.5% and 3% declining rates show decline in net land change by 30% and 50 %, respectively. Sediment decline is another environmental driver that controls either the created subdelta by a sediment diversion thrives or diminishes. The land change results presented in Fig. 9 and tabulated in Table 4 are concerning because they suggest that sediment diversions may not be able to keep up with the pace of land loss if sediment supply continues to decline. This is especially problematic given that sediment supply is projected to decline by 70–90% in the Mississippi River by 2100. The results of this study also highlight the importance of considering the impact of sediment decline when planning restoration projects. If sediment diversions are to be effective, they must be designed to account for the projected decline in sediment supply. This may involve using larger diversions, diverting water to different locations, or using different types of diversions. In addition to the impact on sediment diversions, sediment decline is also likely to have a negative impact on coastal wetlands in other ways. For

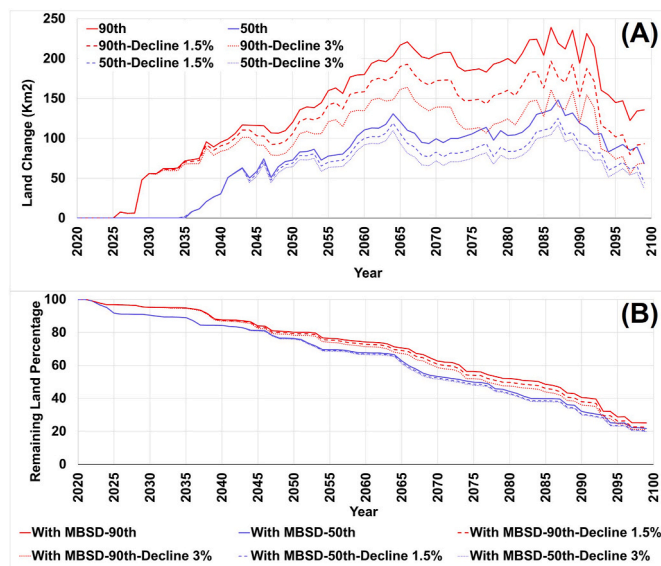


Fig. 9. Modeled land change time series for 1.5% and 3% annual declining sediment scenarios. (A) Land change for different scenarios calculated as remaining marsh from each scenario with MBSD scenario and the corresponding scenario without MBSD scenario. (B) Remaining marsh for different scenarios for both scenarios with and without the MBSD.

Table 4

Tabulated land change by 2100 from different scenarios.

Scenario	Land change (Km ²)
90th Percentile	136
90th Percentile & 1.5% Annual Sediment Reduction	93
90th Percentile & 3% Annual Sediment Reduction	69
75th Percentile	121
50th Percentile	68
50th Percentile & 1.5% Annual Sediment Reduction	44
50th Percentile & 3% Annual Sediment Reduction	37
25th Percentile	53
10th Percentile	9

example, sediment decline can lead to increased erosion, decreased marsh productivity, and increased salinity levels. These impacts are likely to make coastal wetlands more vulnerable to sea level rise and other stressors. It is also important to develop a comprehensive adaptation strategy for coastal wetlands in the face of sediment decline. This strategy should include a variety of measures, such as sediment diversions, marsh creation, and shoreline protection. Overall, the results of this study suggest that sediment decline is a major threat to coastal wetlands and that restoration projects must be designed to account for this threat.

4.4. Limitations and assumptions

The SBM uses a simple marsh classification relation to salinity and inundation developed from CRMS field measurements (Couvillion and Beck, 2013; Snedden et al., 2015; Hiatt et al., 2019; Baustian et al., 2023). It uses one simple marsh collapse mechanism based on inundation (Foster-Martinez et al., 2023). It assumes the succession of each marsh type's seeding, colonization, and production of organic accretion within one growing season (1 year). This study does not account for consolidation or dewatering of fine material deposits that would have significantly affected the results. This study does not account for marsh edge erosion however, it is a very important mechanism for land loss and would have significantly affected the results (Lauzon et al., 2018; Huff et al., 2019; Roy et al., 2020; Reed et al., 2020; Houttuin Bloemendaal et al., 2021; Kalra et al., 2021). Due to the associated uncertainties and

complicated mechanism, the mineral deposition calculation in this study does not account for clay sediment flocculation however, previous studies show the importance of flocculated clay sediment in the land building process (Droppo et al., 2005; Smith and Friedrichs, 2011, 2015; Furukawa et al., 2014; Kemp et al., 2016; Bowers et al., 2017; Fall et al., 2020; Khalifa, 2023). Land subsidence is modeled here using spatially varied subsidence rates with a no temporal change assumption through the simulated period of time (Reed and Yuill, 2017; Byrnes et al., 2019).

5. Summary and conclusions

This study presents a development of a computationally efficient Simplified Biophysical Model (SBM) to evaluate possible restoration strategies. The SBM includes three components, namely hydrodynamic model, morphodynamic model, and marsh inundation module. The hydrodynamic and mineral sediment calculations are performed using the open source Delft3D model. The marsh inundation component of the SBM uses an approximated approach to classify marsh types and to calculate annual organic accretion rates. This simplified approach avoids running a detailed and computationally expensive vegetation model representing various species. While explicit vegetation models are important for detailed ecological studies, they are not critical for studies focusing on decadal landscape evolution and land loss/gain rates. The analysis presented here confirms that the simple SBM is adequate for decadal land loss/gain studies and is computationally efficient. The typical run time for the SBM is ~0.8, 2.5, and 4.7 days real time for one, three, and five decade simulations for an area of 4500 km² defined by 295,400 nodes, respectively which is considered a computationally efficient for modeling decadal landscape evolution. Through the SBM, it is possible to generally represent biophysical interactions simply over decades. The calibrated setup was applied to a set of five experiments from the 240 scenarios presented by Meselhe et al. (2022) to examine the relationship between environmental drivers and land loss rates. The drivers considered in these numerical experiments include SLR rates, subsidence, freshwater inflow, mineral sediment load, and the potential implementation dates of 2025, or 2035 for the proposed MBSD. The SBM captured the landscape evolution with and without the MBSD for the period of 2020 through 2100. As concluded by Meselhe et al. (2022), SLR and operation date are the most two important parameters that distinguish whether the delta created by the MBSD remains or diminishes. Establishing a vegetated surface, as early as possible in the simulation significantly increases the annual elevation gain due to the organic accretion, thereby ameliorating the influence of SLR and subsidence. The sediment reduction analysis confirms the critical impact of the MR sediment decline on potential land building from sediment diversions where 1.5%, and 3% declining rates show decline in net land change due to MBSD operation by 30% and 50 %, respectively. This demonstrates the importance of including the impact of the MR sediment supply decline in restoration projects' planning and specifically, sediment diversions. Overall, this study demonstrates the applicability of the newly developed SBM to model landscape evolution on a decadal basis and to assess coastal restoration strategies. Also, it has the capability to model other deltaic complexes and assess different restoration strategies with the proper tuning parameters to best fit the corresponding environmental drivers for any other deltaic system.

Software availability

Name: Simplified Biophysical Model (SBM).

Developers: Ahmed M. Khalifa, Ehab A. Meselhe, Kelin Hu, Denise Reed, and Md Nazmul Azim Beg.

Contact information: akhalifa1@tulane.edu & emeselhe@tulane.edu.

Hardware required: General-purpose computer.

Programming language: MATLAB.

Availability: The hydrodynamic and morphodynamic models are

open-source and can be accessed via the repository of Deltares (<http://oss.deltares.nl/>). Contact the developers for details about the marsh inundation module.

CRedit authorship contribution statement

Ahmed M. Khalifa: Writing – review & editing, Writing – original draft, Visualization, Validation, Software, Resources, Methodology, Investigation, Formal analysis, Data curation, Conceptualization. **Ehab A. Meselhe:** Writing – review & editing, Writing – original draft, Visualization, Validation, Supervision, Software, Project administration, Methodology, Funding acquisition, Formal analysis, Conceptualization. **Kelin Hu:** Writing – review & editing, Writing – original draft, Visualization, Supervision, Software, Methodology, Formal analysis, Conceptualization. **Denise Reed:** Writing – review & editing, Writing – original draft, Supervision, Resources, Project administration, Methodology, Funding acquisition, Conceptualization. **Md Nazmul Azim Beg:** Writing – original draft, Software, Resources.

Declaration of competing interest

The authors declare that they have no known competing financial interests or personal relationships that could have appeared to influence the work reported in this paper.

Data availability

Data will be made available on request.

Acknowledgements

This work was supported by internal funds from Tulane University and partially by Environmental Defense Fund (EDF). Also, this research was supported, in part, by using high-performance computing (HPC) resources and services provided by both the Louisiana Optical Network Infrastructure (LONI) and Technology Services at Tulane University. We would like to thank Mr. Eric White from CPRA for sharing data used in this analysis. In addition, we would like to thank Dr. Sönke Dangendorf from the department of River-Coastal Science & Engineering at Tulane University for preparing historical eustatic sea level record for the Grand Isle station.

Appendix A. Supplementary data

Supplementary data to this article can be found online at <https://doi.org/10.1016/j.ecss.2024.108899>.

References

- Abutaleb, K.A.A., Mohammed, A.H.E.S., Ahmed, M.H.M., 2018. Climate change impacts, vulnerabilities and adaption measures for Egypt's Nile delta. *Earth Syst. Environ.* 2, 183–192. <https://doi.org/10.1007/s41748-018-0047-9>.
- Allison, M.A., Demas, C.R., Ebersole, B.A., Kleiss, B.A., Little, C.D., Meselhe, E.A., Powell, N.J., Pratt, T.C., Vosburg, B.M., 2012. A water and sediment budget for the lower Mississippi-Atchafalaya River in flood years 2008–2010: implications for sediment discharge to the oceans and coastal restoration in Louisiana. *J. Hydrol.* 432–433, 84–97. <https://doi.org/10.1016/j.jhydrol.2012.02.020>.
- Allison, M.A., Meselhe, E.A., 2010. The use of large water and sediment diversions in the lower Mississippi River (Louisiana) for coastal restoration. *J. Hydrol.* 387, 346–360. <https://doi.org/10.1016/j.jhydrol.2010.04.001>.
- Allison, M.A., Yuill, B.T., Meselhe, E.A., Marsh, J.K., Kolk, A.S., Ameen, A.D., 2017. Observational and numerical particle tracking to examine sediment dynamics in a Mississippi River delta diversion. *Estuar. Coast Shelf Sci.* 194, 97–108. <https://doi.org/10.1016/j.ecss.2017.06.004>.
- Angamuthu, B., Darby, S.E., Nicholls, R.J., 2018. Impacts of natural and human drivers on the multi-decadal morphological evolution of tidally-influenced deltas. *Proc. R. Soc. A Math. Phys. Eng. Sci.* 474 <https://doi.org/10.1098/rspa.2018.0396>.
- Baustian, M.M., Meselhe, E., Jung, H., Sadid, K., Duke-Sylvester, S.M., Visser, J.M., Allison, M.A., Moss, L.C., Ramachandirane, C., Sebastiaan van Maren, D., Jeuken, M., Bargu, S., 2018. Development of an Integrated Biophysical Model to represent morphological and ecological processes in a changing deltaic and coastal ecosystem. *Environ. Model. Softw.* 109, 402–419. <https://doi.org/10.1016/j.envsoft.2018.05.019>.
- Baustian, M.M., Reed, D., Visser, J., Duke-Sylvester, S., Snedden, G., Wang, H., Demarco, K., Foster-Martinez, M., Sharp, L.A., McGinnis, T., Jarrell, E., 2023. ICM-WETLANDS, VEGETATION, and SOILS MODEL IMPROVEMENTS ATTACHMENT D2. Baton Rouge, LA, USA.
- Bevington, A.E., Twilley, R.R., Sasser, C.E., Holm, G.O., 2017. Contribution of river floods, hurricanes, and cold fronts to elevation change in a deltaic floodplain, northern Gulf of Mexico, USA. *Estuar. Coast Shelf Sci.* 191, 188–200. <https://doi.org/10.1016/j.ecss.2017.04.010>.
- Bomer, E.J., Bentley, S.J., Hughes, J.E.T., Wilson, C.A., Crawford, F., Xu, K., 2019. Deltaic morphodynamics and stratigraphic evolution of middle Barataria bay and middle Breton Sound regions, Louisiana, USA: implications for river-sediment diversions. *Estuar. Coast Shelf Sci.* 224, 20–33. <https://doi.org/10.1016/j.ecss.2019.03.017>.
- Bowers, D.G., Mckee, D., Jago, C.F., Nimmo-smith, W.A.M., 2017. Estuarine, Coastal and Shelf Science the area-to-mass ratio and fractal dimension of marine floccs. *Estuar. Coast Shelf Sci.* 189, 224–234. <https://doi.org/10.1016/j.ecss.2017.03.026>.
- Brakenhoff, L., Schrijvershof, R., van der Werf, J., Grasmeyer, B., Ruessink, G., van der Vegt, M., 2020. From ripples to large-scale sand transport: the effects of bedform-related roughness on hydrodynamics and sediment transport patterns in delft3d. *J. Mar. Sci. Eng.* 8, 1–25. <https://doi.org/10.3390/jmse8110892>.
- Byrnes, M.R., Britsch, L.D., Berlinghoff, J.L., Johnson, R., Khalil, S., 2019. Recent subsidence rates for Barataria Basin, Louisiana. *Geo Mar. Lett.* 39, 265–278. <https://doi.org/10.1007/s00367-019-00573-3>.
- Cahoon, D.R., Reed, D.J., 1995. Relationships among marsh surface topography, hydroperiod, and soil accretion in a deteriorating Louisiana salt marsh. *J. Coast Res.* 11, 357–369.
- Caldwell, R.L., Edmonds, D.A., 2014. The effects of sediment properties on deltaic processes and morphologies: a numerical modeling study. *J. Geophys. Res. Earth Surf.* 119, 961–982. <https://doi.org/10.1002/2013JF002965>.
- Chen, Z., Xu, H., Wang, Y., 2021. Ecological degradation of the Yangtze and Nile delta-estuaries in response to dam construction with special reference to monsoonal and arid climate settings. *Water (Switzerland)* 13, 1–10. <https://doi.org/10.3390/w13091145>.
- Collins, D.B.G., Bras, R.L., 2004. Modeling the effects of vegetation-erosion coupling on landscape evolution. *J. Geophys. Res.* 109, 1–11. <https://doi.org/10.1029/2003jf000028>.
- Couvillion, B., 2017. Coastal Protection and Restoration Authority Attachment C3-27: Landscape Data Report: Final. Baton Rouge, LA, USA.
- Couvillion, B., Beck, H., Schoolmaster, D., Fischer, M., 2017. Land Area Change in Coastal Louisiana (1932 to 2016). USGS. <https://doi.org/10.3133/sim3381>.
- Couvillion, B.R., Beck, H., 2013. Marsh collapse thresholds for coastal Louisiana estimated using elevation and vegetation index data. *J. Coast Res.* 63, 58–67. <https://doi.org/10.2112/SI63-006.1>.
- CPRA, 2023. Louisiana's Comprehensive Master Plan for a Sustainable Coast. Baton Rouge, LA, USA.
- CPRA, 2017. Louisiana's Comprehensive Master Plan for a Sustainable Coast. Baton Rouge, LA, USA.
- Crossland, C.J., Kremer, H.H., Lindeboom, H.J., Marshall Crossland, J.I., Le Tissier, M.D., 2005. Coastal fluxes in the anthropocene. *The Land-Ocean Interactions in the Coastal Zone Project of the International Geosphere-Biosphere Programme*. Springer.
- D'Alpaos, A., Lanzoni, S., Mudd, S.M., Fagherazzi, S., 2006. Modeling the influence of hydroperiod and vegetation on the cross-sectional formation of tidal channels. *Estuar. Coast Shelf Sci.* 69, 311–324. <https://doi.org/10.1016/j.ecss.2006.05.002>.
- Dangendorf, S., Hendricks, N., Sun, Q., Klinck, J., Ezer, T., Frederikse, T., Calafat, F.M., Wahl, T., Törnqvist, T.E., 2023. Acceleration of U.S. Southeast and Gulf coast sea-level rise amplified by internal climate variability. *Nat. Commun.* 14, 1935. <https://doi.org/10.1038/s41467-023-37649-9>.
- David, C.H., Maidment, D.R., Niu, G.Y., Yang, Z.L., Habets, F., Eijkhout, V., 2011. River network routing on the NHDplus dataset. *J. Hydrometeorol.* 12, 913–934. <https://doi.org/10.1175/2011JHM1345.1>.
- Dokka, R.K., Sella, G.F., Dixon, T.H., 2006. Tectonic control of subsidence and southward displacement of southeast Louisiana with respect to stable North America. *Geophys. Res. Lett.* 33, 1–5. <https://doi.org/10.1029/2006GL027250>.
- Droppo, I.G., Nackaerts, K., Walling, D.E., Williams, N., 2005. Can floccs and water stable soil aggregates be differentiated within fluvial systems? *Catena* 60, 1–18.
- Edmonds, D.A., Slingerland, R.L., 2007. Mechanics of river mouth bar formation: implications for the morphodynamics of delta distributary networks. *J. Geophys. Res. Earth Surf.* 112 <https://doi.org/10.1029/2006JF000574>.
- Edmonds, D.A., Toby, S.C., Siverd, C.G., Twilley, R., Bentley, S.J., Hagen, S., Xu, K., 2023. Land loss due to human-altered sediment budget in the Mississippi River Delta. *Nat. Sustain.* <https://doi.org/10.1038/s41893-023-01081-0>.
- Elias, E.P.L., 1999. The egmond model - calibration. Validation and Evaluation of Delft3D-MOR with Field Measurements. Delft University of Technology, Delft, the Netherlands.
- Elias, E.P.L., Walstra, D.J.R., Roelvink, D.J.A., Stive, M.J.F., Klein, M.D., 2001. Hydrodynamic validation of Delft3D with field measurements at Egmond. In: *Coastal Engineering 2000 - Proceedings of the 27th International Conference on Coastal Engineering*, ICCE 2000. [https://doi.org/10.1061/40549\(276\)212](https://doi.org/10.1061/40549(276)212).
- Fall, K.A., Friedrichs, C.T., Massey, G.M., Bowers, D.G., Smith, J.S., 2020. The importance of organic content to fractal floc properties in estuarine surface waters: insights from video, LISST, and pump sampling. *J. Geophys. Res. Ocean.* 1–25. <https://doi.org/10.1029/2020JC016787>.

- Foster-Martinez, M., White, E., Jarrell, E., Reed, D., Visser, J., 2023. 2023 Coastal Master Plan: Attachment C8: Modeling Wetland Vegetation and Morphology: ICM-LAVegMod and ICM-Morph. Version 2. Baton Rouge, LA, USA.
- Furukawa, Y., Reed, A.H., Zhang, G., 2014. Effect of organic matter on estuarine flocculation: a laboratory study using montmorillonite, humic acid, xanthan gum, guar gum and natural estuarine flocs. *Geochem. Trans.* 15, 1–9.
- Gaweesh, A., Meselhe, E., 2016. Evaluation of sediment diversion design attributes and their impact on the capture efficiency. *J. Hydraul. Eng.* 142, 4016002 [https://doi.org/10.1061/\(asce\)hy.1943-7900.0001114](https://doi.org/10.1061/(asce)hy.1943-7900.0001114).
- Gourgue, O., Van Belzen, J., Schwarz, C., Vandenbruwaene, W., Vanlede, J., Belliard, J. P., Fagherazzi, S., Bouma, T.J., Van De Koppel, J., Temmerman, S., 2022. Biogeomorphic modeling to assess the resilience of tidal-marsh restoration to sea level rise and sediment supply. *Earth Surf. Dyn.* 10, 531–553. <https://doi.org/10.5194/esurf-10-531-2022>.
- Hiatt, M., Snedden, G., Day, J.W., Rohli, R.V., Nyman, J.A., Lane, R., Sharp, L.A., 2019. Drivers and impacts of water level fluctuations in the Mississippi River delta: implications for delta restoration. *Estuar. Coast Shelf Sci.* 224, 117–137. <https://doi.org/10.1016/j.ecss.2019.04.020>.
- Houttuijn Bloemendaal, L.J., FitzGerald, D.M., Hughes, Z.J., Novak, A.B., Phippen, P., 2021. What controls marsh edge erosion? *Geomorphology* 386. <https://doi.org/10.1016/j.geomorph.2021.107745>.
- Hu, K., Chen, Q., Wang, H., 2015. A numerical study of vegetation impact on reducing storm surge by wetlands in a semi-enclosed estuary. *Coast. Eng.* 95, 66–76. <https://doi.org/10.1016/j.coastaleng.2014.09.008>.
- Hu, K., Meselhe, E., Rhode, R., Snider, N., Renfro, A., 2022. The impact of levee openings on storm surge: a numerical analysis in coastal Louisiana. *Appl. Sci.* 12, 10884 <https://doi.org/10.3390/app122110884>.
- Hu, K., Meselhe, E.A., Reed, D.J., 2023. Understanding drivers of salinity and temperature dynamics in Barataria Basin, Louisiana. *J. Geophys. Res. Ocean.* 128 <https://doi.org/10.1029/2023JC019635>.
- Hu, Z., Borsje, B.W., van Belzen, J., Willemssen, P.W.J.M., Wang, H., Peng, Y., Yuan, L., De Dominicis, M., Wolf, J., Temmerman, S., Bouma, T.J., 2021. Mechanistic modeling of marsh seedling establishment provides a positive outlook for coastal wetland restoration under global climate change. *Geophys. Res. Lett.* 48, 1–12. <https://doi.org/10.1029/2021GL095596>.
- Huff, T.P., Feagin, R.A., Delgado, A.J., 2019. Understanding lateral marsh edge erosion with terrestrial laser scanning (TLS). *Remote Sens.* 11. <https://doi.org/10.3390/rs11192208>.
- Huu Nguyen, H., Dargusch, P., Moss, P., Tran, D.B., 2016. A review of the drivers of 200 years of wetland degradation in the Mekong Delta of Vietnam. *Reg. Environ. Change* 16, 2303–2315. <https://doi.org/10.1007/s10113-016-0941-3>.
- Jankowski, K., Reed, D.J., 2021. Determining Subsidence Rates for Use in Predictive Modeling.
- Kalra, T.S., Ganju, N.K., Aretxabaleta, A.L., Carr, J.A., Defne, Z., Moriarty, J.M., 2021. Modeling marsh dynamics using a 3-D coupled wave-flow-sediment model. *Front. Mar. Sci.* 8 <https://doi.org/10.3389/fmars.2021.740921>.
- Kemp, G.P., Day, J.W., Rogers, J.D., Giosan, L., Peyronnin, N., 2016. Enhancing mud supply from the lower Missouri river to the Mississippi River Delta USA: dam bypassing and coastal restoration. *Estuar. Coast Shelf Sci.* 183, 304–313. <https://doi.org/10.1016/j.ecss.2016.07.008>.
- Khalifa, A.M., 2023. Development and Applications of Morphodynamic Model to Study Deltaic and Coastal Ecosystems. Tulane University, Dissertation.
- Kirwan, M., Temmerman, S., 2009. Coastal marsh response to historical and future sea-level acceleration. *Quat. Sci. Rev.* 28, 1801–1808. <https://doi.org/10.1016/j.quascirev.2009.02.022>.
- Kirwan, M.L., Guntenspergen, G.R., D'Alpaos, A., Morris, J.T., Mudd, S.M., Temmerman, S., 2010. Limits on the adaptability of coastal marshes to rising sea level. *Geophys. Res. Lett.* 37, 1–5. <https://doi.org/10.1029/2010GL045489>.
- Kleiss, B.A., Murphy, J.C., Mayne, C.M., Allgeier, J.P., Edmondson, A.B., Ginsberg, K.C., Jones, K.E., Lauth, T.J., Moe, E.L., Murphy, J.W., Allison, M.A., 2021. Incorporating water quality analysis into navigation assessments as demonstrated in the Mississippi River Basin. *J. Waterw. Port, Coast. Ocean Eng.* 147 [https://doi.org/10.1061/\(asce\)ww.1943-5460.0000651](https://doi.org/10.1061/(asce)ww.1943-5460.0000651).
- Lauzon, R., Murray, A.B., 2022. Discharge determines avulsion regime in model experiments with vegetated and unvegetated deltas. *J. Geophys. Res. Earth Surf.* 127, 1–19. <https://doi.org/10.1029/2021JF006225>.
- Lauzon, R., Murray, A.B., Moore, L.J., Walters, D.C., Kirwan, M.L., Fagherazzi, S., 2018. Effects of marsh edge erosion in coupled barrier island-marsh systems and geometric constraints on marsh evolution. *J. Geophys. Res. Earth Surf.* 123, 1218–1234. <https://doi.org/10.1029/2017JF004530>.
- Lesser, G.R., Roelvink, J.A., van Kester, J.A.T.M., Stelling, G.S., 2004. Development and validation of a three-dimensional morphological model. *Coast. Eng.* 51, 883–915. <https://doi.org/10.1016/j.coastaleng.2004.07.014>.
- Lewis, J.W., Tavakoly, A.A., Martin, C.A., Moore, C.D., 2019. Mississippi River and Tributaries Future Flood Conditions.
- Liang, X., Lettenmaier, D.P., Wood, E.F., Burges, S.J., 1994. A simple hydrologically based model of land surface water and energy fluxes for general circulation models. *J. Geophys. Res.* 99 <https://doi.org/10.1029/94jd00483>.
- Luijendijk, A., 2001. Validation, Calibration and Evaluation of a Delft3D-FLOW Model with Ferry Measurements. Delft University of Technology, Delft, the Netherlands.
- Meade, R.H., Moody, J.A., 2010. Causes for the decline of suspended-sediment discharge in the Mississippi River system, 1940–2007. *Hydrol. Process.* 24, 35–49. <https://doi.org/10.1002/hyp.7477>.
- Meselhe, E., Baustian, M.M., Allison, M., 2015. Basin Wide Model Development for the Louisiana Coastal Area mississippi River Hydrodynamic and Delta Management Study. Baton Rouge, LA, USA.
- Meselhe, E., Khalifa, A.M., Hu, K., Lewis, J., Tavakoly, A.A., 2022. Influence of key environmental drivers on the performance of sediment diversions. *Water (Switzerland)* 14. <https://doi.org/10.3390/w14101024>.
- Meselhe, E., Sadid, K., Khadka, A., 2021a. Sediment distribution, retention and morphodynamic analysis of a river-dominated deltaic system. *Water* 13, 1341. <https://doi.org/10.3390/w13101341>.
- Meselhe, E., Sadid, K.M., Allison, M.A., 2016. Riverside morphological response to pulsed sediment diversions. *Geomorphology* 270, 184–202. <https://doi.org/10.1016/j.geomorph.2016.07.023>.
- Meselhe, E., White, E., Wang, Y., Reed, D., 2021b. Uncertainty analysis for landscape models used for coastal planning. *Estuar. Coast Shelf Sci.* 256 <https://doi.org/10.1016/j.ecss.2021.107371>.
- Mize, S.V., Murphy, J.C., Diehl, T.H., Demcheck, D.K., 2018. Suspended-sediment concentrations and loads in the lower Mississippi and Atchafalaya rivers decreased by half between 1980 and 2015. *J. Hydrol.* 564, 1–11. <https://doi.org/10.1016/j.jhydrol.2018.05.068>.
- Morgan, J.A., Kumar, N., Horner-Devine, A.R., Ahrendt, S., Istanbuloglu, E., Bandaragoda, C., 2020. The use of a morphological acceleration factor in the simulation of large-scale fluvial morphodynamics. *Geomorphology* 356. <https://doi.org/10.1016/j.geomorph.2020.107088>.
- Mossa, J., 1996. Sediment dynamics in the lowermost Mississippi River. *Eng. Geol.* 45, 457–479.
- Mukai, A.Y., Westerink, J.J., Luetlich, R.A., Mark, D., York, N., 2002. Eastcoast 2001, A Tidal Constituent Database for Western North Atlantic, Gulf of Mexico, and Caribbean Sea.
- Palaseanu-Lovejoy, M., Kranenburg, C., Barras, J.A., Brock, J.C., 2013. Land loss due to recent hurricanes in Coastal Louisiana, U.S.A. *J. Coast Res.* 63, 97–109. <https://doi.org/10.2112/Si63-009.1>.
- Parker, A., 2020. Anthropogenic Drivers of Relative Sea-Level Rise in the Mekong Delta - A Review. *Quaest. Geogr.* 39, 109–124. <https://doi.org/10.2478/quageo-2020-0009>.
- Partheniades, E., 1965. Erosion and Deposition of Cohesive Soils. *J. Hydraul. Div.* 91.
- Peyronnin, N.S., Caffey, R.H., Cowan, J.H., Justic, D., Kolker, A.S., Laska, S.B., McCorquodale, A., Melancon, E., Nyman, J.A., Twilley, R.R., Visser, J.M., White, J. R., Wilkins, J.G., 2017. Optimizing sediment diversion operations: Working group recommendations for integrating complex ecological and social landscape interactions. *Water (Switzerland)* 9. <https://doi.org/10.3390/w9060368>.
- PSMSL, 2022. Permanent Service for Mean Sea Level [WWW Document]. URL. <https://psmsl.org/data/obtaining/stations/526.php>.
- Ramakrishnan, B., Pratap Singh, N., Jeyaraj, S., 2019. Input reduction and acceleration techniques in a morphodynamic modeling: A case study of Mumbai harbor. *Reg. Stud. Mar. Sci.* 31 <https://doi.org/10.1016/j.risma.2019.100765>.
- Rebich, R.A., Demcheck, D.K., 2007. Trends in Nutrient and Sediment Concentrations and Loads in Major River Basins of the South-Central United States, pp. 1993–2004. Reston, Virginia.
- Reed, D., Wang, Y., Meselhe, E., White, E., 2020. Modeling wetland transitions and loss in coastal Louisiana under scenarios of future relative sea-level rise. *Geomorphology*. <https://doi.org/10.1016/j.geomorph.2019.106991>.
- Reed, D., Yuill, B., 2017. Coastal Protection and Restoration Authority Attachment C2-2: Subsidence Report: Final. Baton Rouge, LA, USA.
- Reed, D.J., Cahoon, D.R., 1992. The relationship between marsh surface topography, hydroperiod, and growth of *Spartina alterniflora* in a deteriorating Louisiana salt marsh. *J. Coast Res.* 8, 77–87.
- Rego, J.L., Meselhe, E., Stronach, J., Habib, E., 2010. Numerical modeling of the Mississippi-at-chafalaya rivers' sediment transport and fate: Considerations for diversion scenarios. *J. Coast Res.* 26, 212–229. <https://doi.org/10.2112/08-1072.1>.
- Reyns, J., Dastgheib, A., Ranasinghe, R., Luijendijk, A., Walstra, D.-J., Roelvink, D., 2014. Morphodynamic upscaling with the morfac approach in tidal conditions: the critical morfac. *Coast. Eng.* 1, 34. <https://doi.org/10.9753/icce.v34.sediment.27>.
- Roelvink, J.A., 2006. Coastal morphodynamic evolution techniques. *Coast. Eng.* 53, 277–287. <https://doi.org/10.1016/j.coastaleng.2005.10.015>.
- Roy, S., Robeson, S.M., Ortiz, A.C., Edmonds, D.A., 2020. Spatial and temporal patterns of land loss in the Lower Mississippi River Delta from 1983 to 2016. *Remote Sens. Environ.* 250 <https://doi.org/10.1016/j.rse.2020.112046>.
- Rozas, L.P., Reed, D.J., 1993. Nekton use of marsh-surface habitats in Louisiana (USA) deltaic salt marshes undergoing submergence. *Mar. Ecol. Prog. Ser.* <https://doi.org/10.3354/meps096147>.
- Sandén, A.B., Donselaar, M.E., Storms, J.E.A., Van Toorenburg, K.A., Van Der Vegt, H., Weltje, G.J., 2016. Process-based modelling of sediment distribution in fluvial crevasse splays validated by outcrop data. In: 2nd Conference on Forward Modelling of Sedimentary Systems: from Desert to Deep Marine Depositioned Systems. European Association of Geoscientists and Engineers, EAGE, pp. 23–27. <https://doi.org/10.3997/2214-4609.201600359>.
- Scaife, W.W., Turner, R.E., Costanza, R., 1983. Coastal Louisiana recent land loss and canal impacts. *Environ. Manage.* 7, 433–442. <https://doi.org/10.1007/BF01867123>.
- Schuerch, M., Vafeidis, A., Slawig, T., Temmerman, S., 2013. Modeling the influence of changing storm patterns on the ability of a salt marsh to keep pace with sea level rise. *J. Geophys. Res. Earth Surf.* 118, 84–96. <https://doi.org/10.1029/2012JF002471>.
- Sendrowski, A., Sadid, K., Meselhe, E., Wagner, W., Mohrig, D., Passalacqua, P., 2018. Transfer entropy as a tool for hydrodynamic model validation. *Entropy* 20. <https://doi.org/10.3390/e20010058>.
- Shinkle, K.D., Dokka, R.K., 2004. Rates of Vertical Displacement at Benchmarks in the Lower Mississippi Valley and the Northern Gulf Coast. NOAA Technical Report 50.

- Smith, S.J., Friedrichs, C.T., 2015. Image processing methods for in situ estimation of cohesive sediment floc size, settling velocity, and density. *Limnol Oceanogr. Methods* 13, 250–264. <https://doi.org/10.1002/lom3.10022>.
- Smith, S.J., Friedrichs, C.T., 2011. Size and settling velocities of cohesive flocs and suspended sediment aggregates in a trailing suction hopper dredge plume. *Continent. Shelf Res.* 31 <https://doi.org/10.1016/j.csr.2010.04.002>.
- Snedden, G.A., Cretini, K., Patton, B., 2015. Inundation and salinity impacts to above- and belowground productivity in *Spartina patens* and *Spartina alterniflora* in the Mississippi River deltaic plain: Implications for using river diversions as restoration tools. *Ecol. Eng.* 81, 133–139. <https://doi.org/10.1016/j.ecoleng.2015.04.035>.
- Stark, J., Plancke, Y., Ides, S., Meire, P., Temmerman, S., 2016. Coastal flood protection by a combined nature-based and engineering approach: Modeling the effects of marsh geometry and surrounding dikes. *Estuar. Coast Shelf Sci.* 175, 34–45. <https://doi.org/10.1016/j.ecss.2016.03.027>.
- Sušnik, J., Vamvakieridou-Lyroudia, L.S., Baumert, N., Kloos, J., Renaud, F.G., La Jeunesse, I., Mabrouk, B., Savić, D.A., Kapelan, Z., Ludwig, R., Fischer, G., Roson, R., Zografos, C., 2015. Interdisciplinary assessment of sea-level rise and climate change impacts on the lower Nile delta, Egypt. *Sci. Total Environ.* 503–504, 279–288. <https://doi.org/10.1016/j.scitotenv.2014.06.111>.
- Syvitski, J.P.M., Kettner, A.J., Overeem, I., Hutton, E.W.H., Hannon, M.T., Brakenridge, G.R., Day, J., Vörösmarty, C., Saito, Y., Giosan, L., Nicholls, R.J., 2009. Sinking deltas due to human activities. *Nat. Geosci.* 2, 681–686. <https://doi.org/10.1038/ngeo629>.
- Takagi, H., Thao, N.D., Anh, L.T., 2016. Sea-level rise and land subsidence: Impacts on flood projections for the Mekong Delta's largest city. *Sustain. Times* 8, 1–15. <https://doi.org/10.3390/su8090959>.
- Tavakoly, A.A., Snow, A.D., David, C.H., Follum, M.L., Maidment, D.R., Yang, Z.L., 2017. Continental-Scale River Flow Modeling of the Mississippi River Basin Using High-Resolution NHDPlus Dataset. *J. Am. Water Resour. Assoc.* 53, 258–279. <https://doi.org/10.1111/1752-1688.12456>.
- Temmerman, S., Govers, G., Meire, P., Wartel, S., 2003. Modelling long-term tidal marsh growth under changing tidal conditions and suspended sediment concentrations, Scheldt estuary, Belgium. *Mar. Geol.* 193, 151–169. [https://doi.org/10.1016/S0025-3227\(02\)00642-4](https://doi.org/10.1016/S0025-3227(02)00642-4).
- Temmerman, S., Govers, G., Wartel, S., Meire, P., 2004. Modelling estuarine variations in tidal marsh sedimentation: Response to changing sea level and suspended sediment concentrations. *Mar. Geol.* 212, 1–19. <https://doi.org/10.1016/j.margeo.2004.10.021>.
- Thanh, Q.V., 2021. MODELING OF HYDRODYNAMICS AND SEDIMENT TRANSPORT IN THE MEKONG DELTA. Delft University of Technology, Delft, the Netherlands.
- USACE, 2020. Mid-Barataria Sediment Diversion Project EIS Appendix E: Delft3D Basinwide Modeling. New Orleans.
- Van Rijn, L.C., 2007. Unified View of Sediment Transport by Currents and Waves. I: Initiation of Motion, Bed Roughness, and Bed-Load Transport. *J. Hydraul. Eng.* 133, 649–667. <https://doi.org/10.1061/ASCE0733-94292007133:6649>.
- Visser, J.M., Duke-Sylvester, S.M., 2017. LaVegMod v2: Modeling coastal vegetation dynamics in response to proposed coastal restoration and protection projects in Louisiana, USA. *Sustain. Times* 9. <https://doi.org/10.3390/su9091625>.
- Vu, D.T., Yamada, T., Ishidaira, H., 2018. Assessing the impact of sea level rise due to climate change on seawater intrusion in Mekong Delta, Vietnam. *Water Sci. Technol.* 77, 1632–1639. <https://doi.org/10.2166/wst.2018.038>.
- Wang, H., Steyer, G.D., Couvillion, B.R., Rybczyk, J.M., Beck, H.J., Sleavin, W.J., Meselhe, E.A., Allison, M.A., Boustany, R.G., Fischenich, C.J., Rivera-Monroy, V.H., 2014. Forecasting landscape effects of Mississippi River diversions on elevation and accretion in Louisiana deltaic wetlands under future environmental uncertainty scenarios. *Estuar. Coast Shelf Sci.* 138, 57–68. <https://doi.org/10.1016/j.ecss.2013.12.020>.
- Wang, H., Waldon, M.G., Meselhe, E.A., Arceneaux, J.C., Chen, C., Harwell, M.C., 2009. Surface Water Sulfate Dynamics in the Northern Florida Everglades. *J. Environ. Qual.* 38, 734–741. <https://doi.org/10.2134/jeq2007.0455>.
- Wasklewicz, T., Zhu, Z., Gares, P., 2017. Simulating and quantifying legacy topographic data uncertainty: An initial step to advancing topographic change analyses. *Prog. Earth Planet. Sci.* 4.
- White, E.D., Meselhe, E., Reed, D., Renfro, A., Snider, N.P., Wang, Y., 2019a. Mitigating the effects of sea-level rise on estuaries of the Mississippi Delta Plain using river diversions. *Water (Switzerland)* 11. <https://doi.org/10.3390/w11102028>.
- White, E.D., Reed, D.J., Meselhe, E.A., 2019b. Modeled Sediment Availability, Deposition, and Decadal Land Change in Coastal Louisiana Marshes under Future Relative Sea Level Rise Scenarios. *Wetlands* 39, 1233–1248. <https://doi.org/10.1007/s13157-019-01151-0>.
- Xing, F., Meselhe, E.A., Allison, M.A., Weathers, H.D., 2017. Analysis and numerical modeling of the flow and sand dynamics in the lower Song Hau channel, Mekong Delta. *Continent. Shelf Res.* 147, 62–77. <https://doi.org/10.1016/j.csr.2017.08.003>.
- Yuill, B., Lavoie, D., Reed, D.J., 2009. Understanding Subsidence Processes in Coastal Louisiana. *J. Coast Res.* 10054, 23–36. <https://doi.org/10.2112/si54-012.1>.
- Yuill, B.T., Khadka, A.K., Pereira, J., Allison, M.A., Meselhe, E.A., 2016. Morphodynamics of the erosional phase of crevasse-splay evolution and implications for river sediment diversion function. *Geomorphology* 259, 12–29. <https://doi.org/10.1016/j.geomorph.2016.02.005>.